AGU PUBLICATIONS

JGR

Journal of Geophysical Research: Biogeosciences

RESEARCH ARTICLE
10.1002/2017JG004284

Key Points:
- Rare earth elements can be used as tracers of aeolian sediment redistribution
- Vegetation microsites, which are sinks of aeolian sediments in arid landscapes, may become active sediment sources following fires
- Postfire acceleration of aeolian processes results in the spatial homogenization of sediment distribution

Supporting Information:
- Supporting Information S1

Correspondence to:
S. Ravi,
sravi@temple.edu

Citation:
Dukes, D., Gonzales, H. B., Ravi, S., Grandstaff, D. E., Van Pelt, R. S., Li, J., … Sankey, J. B. (2018). Quantifying postfire aeolian sediment transport using rare earth element tracers. *Journal of Geophysical Research: Biogeosciences*, *123*, 288–299. https://doi.org/10.1002/2017JG004284

Received 9 NOV 2017
Accepted 10 JAN 2018
Accepted article online 15 JAN 2018
Published online 31 JAN 2018

Quantifying Postfire Aeolian Sediment Transport Using Rare Earth Element Tracers

David Dukes[1], Howell B. Gonzales[1], Sujith Ravi[1], David E. Grandstaff[1], R. Scott Van Pelt[2], Junran Li[3], Guan Wang[3], and Joel B. Sankey[4]

[1]Department of Earth and Environmental Science, Temple University, Philadelphia, PA, USA, [2]Wind Erosion and Water Conservation Research, USDA-ARS, Big Spring, TX, USA, [3]Department of Geosciences, University of Tulsa, Tulsa, OK, USA, [4]Southwest Biological Science Center, Grand Canyon Monitoring and Research Center, U. S. Geological Survey, Flagstaff, AZ, USA

Abstract Grasslands, which provide fundamental ecosystem services in many arid and semiarid regions of the world, are undergoing rapid increases in fire activity and are highly susceptible to postfire-accelerated soil erosion by wind. A quantitative assessment of physical processes that integrates fire-wind erosion feedbacks is therefore needed relative to vegetation change, soil biogeochemical cycling, air quality, and landscape evolution. We investigated the applicability of a novel tracer technique—the use of multiple rare earth elements (REE)—to quantify soil transport by wind and to identify sources and sinks of wind-blown sediments in both burned and unburned shrub-grass transition zone in the Chihuahuan Desert, NM, USA. Results indicate that the horizontal mass flux of wind-borne sediment increased approximately threefold following the fire. The REE tracer analysis of wind-borne sediments shows that the source of the horizontal mass flux in the unburned site was derived from bare microsites (88.5%), while in the burned site it was primarily sourced from shrub (42.3%) and bare (39.1%) microsites. Vegetated microsites which were predominantly sinks of aeolian sediments in the unburned areas became sediment sources following the fire. The burned areas showed a spatial homogenization of sediment tracers, highlighting a potential negative feedback on landscape heterogeneity induced by shrub encroachment into grasslands. Though fires are known to increase aeolian sediment transport, accompanying changes in the sources and sinks of wind-borne sediments may influence biogeochemical cycling and land degradation dynamics. Furthermore, our experiment demonstrated that REEs can be used as reliable tracers for field-scale aeolian studies.

1. Introduction

Population increase; overexploitation of land and water resources; recurrent disturbances such as fire, drought, and overgrazing; and climatic changes have rendered drylands worldwide highly susceptible to land degradation, a phenomenon often referred to as "desertification" (Darkoh, 1998; D'Odorico et al., 2013). Understanding the biophysical and human dimensions of land degradation in drylands is critical because drylands cover at least 40% of the Earth's terrestrial surface and play a fundamental role for food security and environmental quality (MEA, 2005; UNCCD, 1994). Accelerated soil erosion by hydrologic and aeolian processes is thought to be responsible for over 87% of the degraded drylands and is often regarded as a cause and effect of desertification (Lal, 2001; Middleton & Thomas, 1997). At the local scale, accelerated wind erosion results in loss and redistribution of soil resources and mechanical injury to growing plants (Retta et al., 2000; Van Pelt & Zobeck, 2007). The dust emissions have large-scale impacts and affect human health, biogeochemical cycles, precipitation processes, and climate (Field et al., 2010; Ravi et al., 2011). Furthermore, increases in rates of wind erosion and dust emissions resulting from increased aridity (climatic changes) may result in enhanced loss of soil resources and a decline in vegetation cover (Munson et al., 2011; Ravi et al., 2011). As vegetation exerts a dominant control on wind erosion, vegetation shifts (e.g., grass-shrub transitions and exotic grass invasions) and disturbances to vegetation such as wildfires can greatly enhance the transport and redistribution of soil resources by wind (Mayaud et al., 2017; Miller et al., 2012; Sankey et al., 2009, 2013; Whicker et al., 2002).

Grasslands, which provide fundamental ecosystem services in arid and semiarid regions of the world, are undergoing rapid increases in fire activity and are highly susceptible to postfire-accelerated soil erosion by wind (Bowman et al., 2009; Ravi et al., 2012). A common form of land degradation in many drylands is the encroachment of woody plants into areas historically dominated by grasses. This phenomenon is observed

worldwide and is often referred to as "shrub encroachment" (Ravi et al., 2009; Schlesinger et al., 1990). Several studies have investigated the ecohydrological, geomorphological, and biogeochemical implications of this transformative ecosystem change (Huxman et al., 2005; Li et al., 2007, 2008; Turnbull et al., 2012). Shrub encroachment is thought to contribute to land degradation by increasing the amount of bare soil which can be eroded by wind (Gillette & Pitchford, 2004; Okin & Gillette, 2001) and allows for sediment and soil nutrients to be stripped from unvegetated areas and partially redistributed via canopy trapping onto shrub patches (Li et al., 2008; Schlesinger et al., 1990). This creates a self-sustaining cycle of erosion, depletion of soil nutrients, and loss of grass cover (Archer et al., 1995). The loss of grasses decreases connectivity between vegetated sites and thus decreases the pressure of fires on shrub vegetation further enhancing woody plant encroachment (Archer et al., 1995; Van Auken, 2000). The resulting heterogeneous landscape is characterized by topographically raised, hydrologically and nutritionally enhanced shrub islands (or "islands of fertility"), which are sediment sinks, and deflated, nutrient depleted bare interspaces that act as sediment sources (Schlesinger et al., 1990).

Fires are common in many shrub-grass transition systems, and important feedbacks are known to exist among wind transport, soil erosion, vegetation change, and fires (Li et al., 2007, 2008; Sankey et al., 2009; Sankey, Germino, Sankey, & Hoover, 2012). In the grass-shrub ecotones of the Chihuahuan Desert in the southwestern United States, recent studies have demonstrated that by altering soil erosion processes at the early stages of shrub encroachment, fires can play an important role in the local-scale redistribution of soil resources within the landscape (Sankey, Ravi, et al., 2012; Van Pelt et al., 2017). On low-relief surfaces, fires can induce rapid changes in soil surface characteristics, remove vegetation cover, and increase erosion and sediment redistribution (Paysen et al., 2000; Ravi et al., 2009; Whicker et al., 2002). Furthermore, burning of vegetative biomass at the surface can induce soil water repellency, which has been shown to enhance postfire soil erosion by decreasing the interparticle forces due to moisture in soils (DeBano, 1966; Ravi et al., 2006, 2007). Recent studies using wind tunnels and small-scale field experiments have qualitatively demonstrated that in shrublands and shrub-grass transition zones fires can enhance soil erosion under raised shrub vegetated microsites (i.e., small-scale patches representing the different surface cover types) and result in some level of sediment redistribution to the deflated interspaces (Ravi et al., 2009; Sankey, Germino, & Glenn, 2012; Sankey, Germino, Sankey, & Hoover, 2012; Sankey, Ravi, et al., 2012; White et al., 2006). Modeling studies have indicated that shrub recruitment and growth at an early stage of encroachment can be controlled with lower grazing intensity and recurrent prescribed or natural fires (Ravi & D'Odorico, 2009). The natural fire return intervals for North American desert grasslands like the Chihuahuan Desert have been estimated to be around 7–10 years to sustain grass dominance (McPherson, 1995; White & Swint, 2014). Hence, recurrent prescribed fires can used by land managers to maintain Chihuahuan Desert grasslands and can result in the reduction of shrub cover and redistribution of sediment and nutrients from shrub islands to grass and bare interspaces. This homogenization process may have the potential to shift the shrub-grass transition back to a stable grassland state (D'Odorico et al., 2013; Ravi & D'Odorico, 2009). Even though this fire-erosion feedback has the potential to homogenize the landscape (Sankey et al., 2010; Sankey, Germino, Sankey, & Hoover, 2012; Sankey et al., 2009), the actual extent of postfire soil redistribution and homogenization at the microsite scale is poorly understood. This is a critical research gap, as quantifying the postfire redistribution and loss of sediment and soil resources is important in evaluating the extent of land degradation and effectiveness of grassland management practices.

A quantitative assessment of physical processes such as sediment transport that integrates fire-wind erosion feedbacks is therefore critical for understanding land degradation dynamics, vegetation change, soil biogeochemical cycling, and air quality impacts. However, this quantification is challenging, partly due to the lack of reliable tracer-based techniques to precisely determine the rate of soil transport and redistribution or to reconstruct the aeolian source-to-sink routes (Wang et al., 2017). Several studies have used tracers, such as oxides of rare earth elements (REEs), to quantify water erosion rates (Guzmán et al., 2013; Polyakov & Nearing, 2004; Zhang et al., 2001; Zhu et al., 2011). These studies showed that soil redistribution patterns, erosion and aggregation, can be tracked with REE tracers (Zhang et al., 2001). Wang et al. (2017) provide a comprehensive review on current tracer techniques for aeolian research; however, studies specific to quantifying aeolian transport using REE traces are limited or still in development (e.g., Van Pelt et al., 2012, 2014).

REEs have been proven to be reliable tracers in laboratory settings with limited research focusing on field applications (Deasy & Quinton, 2010; Zhang et al., 2001). Past studies have either physically mixed REE

powders with soil or sprayed water-suspended REE powder on the soil surface (Deasy & Quinton, 2010; Zhang et al., 2001). Preliminary studies which focus on noninvasive tracer applications (no disturbance to existing vegetation or the soil surface) for wind erosion have led to the development of REE application protocols which use dissolved REEs in a calibrated sprayer (Van Pelt et al., 2012, 2014). Similar methods to this study were used for tracking aeolian redistribution of surface sediments from a point source using field wind tunnel studies (Van Pelt et al., 2012, 2014). However, the field scale use of multiple REE tracers for wind erosion studies applied with this method has never been assessed. Here we investigated the applicability of this tracer technique—the novel use of multiple REE tracers to quantify field-scale soil transport by wind and to identify sources and sinks of wind-blown sediments in a fire-affected, desert shrub-grass ecotone. We hypothesize that vegetation microsites (shrub or grass patches), which are sinks of aeolian sediments in arid landscapes, may act as enhanced sediment sources following fires. This postfire modification of sediment sources and sinks in the landscape might impact rates of resource redistribution and soil patterning, leading to an ecogeomorphic shift from a heterogeneous landscape characterized by topographically raised shrub islands of fertility and deflated bare interspaces to a more homogeneous grass-dominated surface. Using multiple REEs as tracers at the field scale, we hope to quantify the components of aeolian fluxes which are sourced from varying surface cover post fire.

2. Materials and Methods

2.1. Study Site

Field experiments were conducted at the Sevilleta National Wildlife Refuge (SNWR) in the northern Chihuahuan Desert approximately 80 km south of Albuquerque, New Mexico. The shrub-grass transition zone (latitude/longitude: 34.33062°N, 106.72078°W) is a heterogeneous landscape with a mosaic of black grama grass (Bouteloua eriopoda (Torr.) Torr.) and creosote shrub (*Larrea tridentata* (DC.) Cov.) with bare soil interspaces. The land cover in the study area is typical of shrub-encroached desert grassland, with about 70–75% grass cover, 20–30% bare interspaces, and a low density (5–10%) of shrubs (Báez & Collins, 2008). In the field site, grasses provide enough connectivity among shrub patches to allow the fire spread in the presence of strong winds (Ravi et al., 2009). The windy season in this area is from February to May, and the predominant wind is from the southwest (Ravi et al., 2009). Most precipitation occurs from June to October, during the North American monsoon (Higgins et al., 1997). The soil in the study area is primarily sandy loam (Johnson, 1988).

2.2. Experimental Setup

The experimental site consisted of two 100 m × 100 m treatment areas, one control (unburned) and one burned, which are 250 m apart and oriented on the northwest-southeast line, perpendicular to the prevailing wind direction (from the southwest) (Figure 1a). The areas were established at the beginning of the windy season in March 2016 and are characterized by similar soil texture, vegetation, and topography. In each treatment area we established three 30 m × 10 m replicate plots (25 m apart) oriented perpendicular to the predominant wind direction. A line transect plant investigation was conducted to ensure that each plot encompassed the complete surface cover heterogeneity of the landscape (i.e., contained shrub, grass, and bare microsites). In the middle of each of the replicated plots, a 5 m × 5 m sampling zone was established to conduct the REE tracer application study. In each sampling zone individual REE tracers were applied to their respective microsite types (shrub, grass, and bare) such that the entire surface of each zone contained REE tracers. The 100 × 100 m burned area was created at the beginning of March using a prescribed fire conducted in one of the monitoring areas (Figure 1b). Prescribed fires were ignited using hydrocarbons on the downwind edge of the experimental (burned) site. After ignition, the grass cover provided enough connectivity among shrub patches to allow for the fire to spread by winds. The fire was restricted inside the target area by creating a control line around the area by removing vegetation. Partially burnt shrubs were subsequently torched to ensure complete removal of vegetation. The postfire landscape consisted of shrub stumps and burned grass pedestals supported by the remaining grass root mass (Figure 1c).

2.3. Wind Transport Monitoring

Aeolian sediment was sampled using custom-made MWAC (Modified Wilson and Cooke) sediment samplers (isokinetic sediment collectors) installed at each monitoring area in order to determine the sediment horizontal mass flux (Q, the major flux responsible for on-site soil redistribution by wind at the plant interspace to near-field scale). Two MWAC samplers were placed at the downwind side of each of the 5 m × 5 m

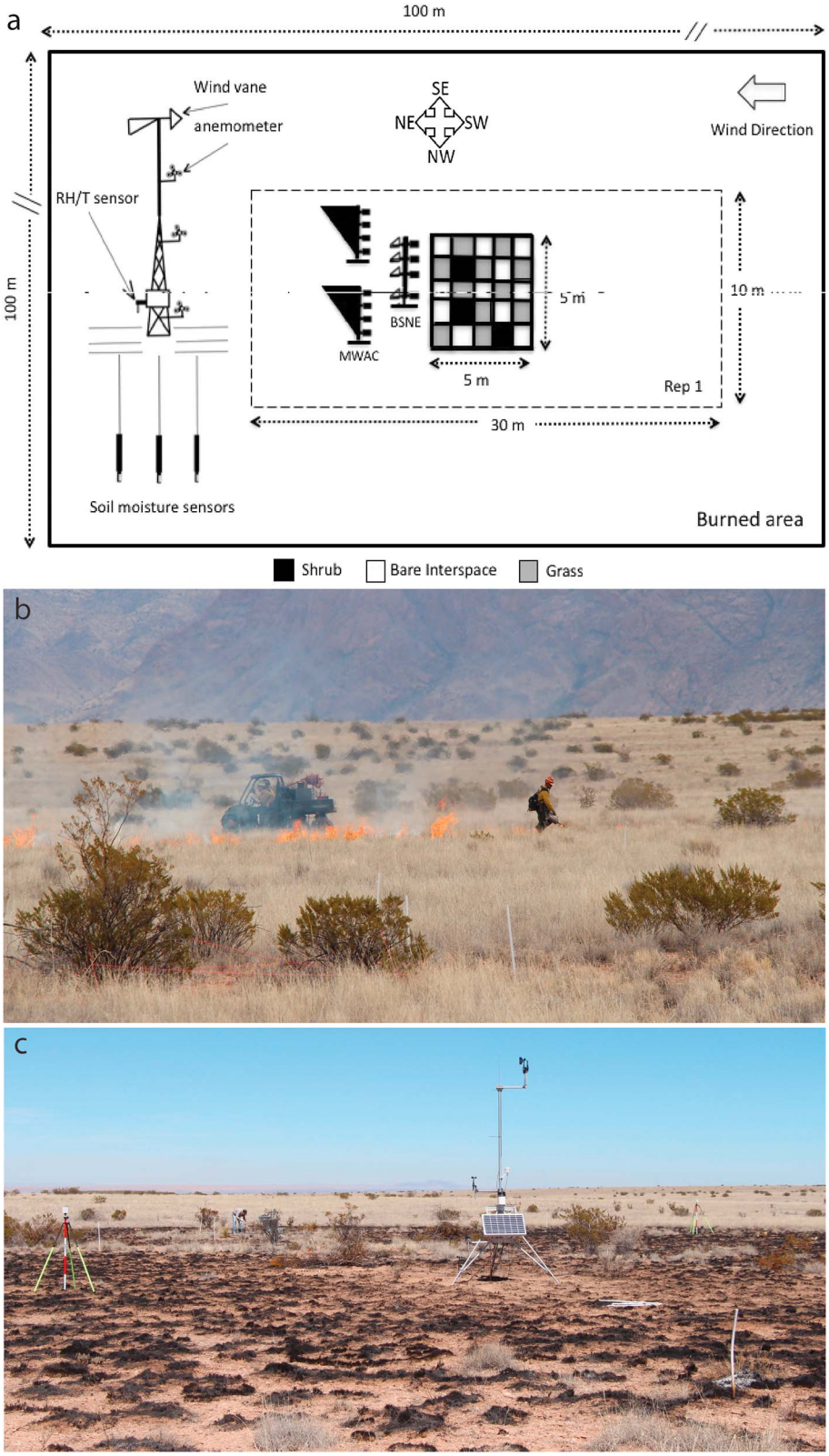

Figure 1. (a) The layout of the burned treatment area (100 × 100 m) is perpendicular to the predominant wind direction (SW) and consists of three replicate plots (30 × 10 m) which each contain a sampling zone (5 × 5 m). The control treatment area is adjacent to the burned treatment area. Neither is downwind from the other. (b) The prescribed fire at the shrub-grass transition zone in Sevilleta National Wildlife Refuge, New Mexico. (c) The postfire landscape with charred shrub stumps and grass pedestals.

sampling zone. The MWAC sampling systems, installed at the beginning of the windy season (March), consist of an array of samplers mounted at four different heights (nominally 0.1, 0.25, 0.5, and 1.0 m above the ground) attached to a pivoting wind vane. The MWACs collected sediment for 90 days over the course of the windy season. During this time, none of the samplers filled to capacity.

The time-averaged specific sediment flux, $q(z)$, was calculated by dividing the mass of sediment collected in the samplers by the collection interval and the area of the MWAC sampler inlet (2.34×10^{-4} m^2). The $q(z)$ results were fit to a widely used empirical formula developed by Shao and Raupach (1992)

$$q(z) = ce^{(az^2+bz)} \quad (1)$$

where z is the height from the ground to the center of the sediment sampler inlet and a, b, and c are fitting constants. The total Q was calculated by integrating $q(z)$ from the ground to a height (H) of 1 m (Bhattachan et al., 2013; Li et al., 2007; Shao & Raupach, 1992; Shao et al., 1993).

$$Q = \int_0^H q(z)\mathrm{d}z \quad (2)$$

Finally, the threshold shear velocity (u_{*t}) of the soil surface among treatment areas and microsites was estimated to evaluate erodibility using a method developed by Li et al. (2010). In this method, u_{*t} were estimated by an empirical equation using the resistance to disturbance created by a penetrometer and projectile shot by an air gun at the soil. Both air gun and penetrometer were applied along a triangle at 45° to the soil surface, and the readings from the penetrometer (kg) and sizes of the surface soil disturbance (length × width) created by the air gun were recorded. This method allowed us to estimate u_{*t} at small surfaces such as the grass microsites. The measurements were conducted along the plant line transects at an interval of every 1 m, and the microsite type (bare, grass, or shrub) of the measurement locations was recorded. More details about this method, including the accuracy of u_{*t} estimates, may be found in Li et al. (2010, 2013).

2.4. Rare Earth Element Tracers

REE oxides have a strong binding capability, low mobility, low background concentrations in soils, low environmental toxicity, and multiple REEs allow for multiple tracers with distinct signatures (Deasy & Quinton, 2010; Kimoto et al., 2006; Polyakov & Nearing, 2004; Zhang et al., 2001). Even though REEs are present in crustal rocks in concentrations similar to metals such as copper and zinc (Haxel et al., 2002), REEs rarely concentrate in ore bodies and tend to only be present as a background element in most soils.

For this study, we implemented the REE application protocols for wind erosion developed by Van Pelt et al. (2012, 2014). At the beginning of March, Holmium oxide (Ho_2O_3), Ytterbium oxide (Yb_2O_3), and Europium oxide (Eu_2O_3) were applied on shrub, bare, and grass microsites, respectively. The choice of REE oxides was determined by their low background concentrations in the soil (0.27 ppm Ho, 1.12 ppm Yb, and 0.26 ppm Eu), availability, and cost. A calculated mass of each REE oxide was dissolved in nitric acid (3 N), diluted with deionized water (for a solution concentration of 2,790 ppm Ho, 5220 ppm Yb, and 1965 ppm Eu), and then sprayed onto microsites in each sampling zone using a calibrated sprayer to ensure a uniform concentration (Deasy & Quinton, 2010; Van Pelt et al., 2012, 2014). The volume sprayed was calculated using the area of each microsite in order for the tracer to penetrate the top 2 cm of the soil profile (Van Pelt et al., 2014). The target spiked concentration was 500 times that of the background concentration.

To determine the background and spiked REE tracer concentrations, 50 randomly distributed samples (10 g each) were taken from the top 2 cm of soil in each (5 m × 5 m) sampling zone before REE application at the beginning of the windy season (March) and after REE oxide application. Samples were taken from the surface of bare microsites and from the pedestal of shrub and grass microsites. Sediment samples were again collected after the windy season 90 days later in June, to assess the depletion and enrichment of REEs in the different microsites. The enrichment or depletion of REE tracers relative to background and spiked REE concentrations in each sampling zone was determined by the Kruskal-Wallis statistical test (NCSS 11, 2016) which compared the concentrations of each REE tracer in each microsite type at time zero and 90 days.

A minimum of 15 samples from each of the three sampling zones (post windy season) within the two treatment areas (burned and control) were analyzed for the concentration of REEs. Of the analyzed burned treatment samples, 32 were from bare sites, 15 were from grass, and 16 were from shrub microsites. From the control area 57 bare, 14 grass, and 10 shrub samples were analyzed. Due to the limited mass of sediment

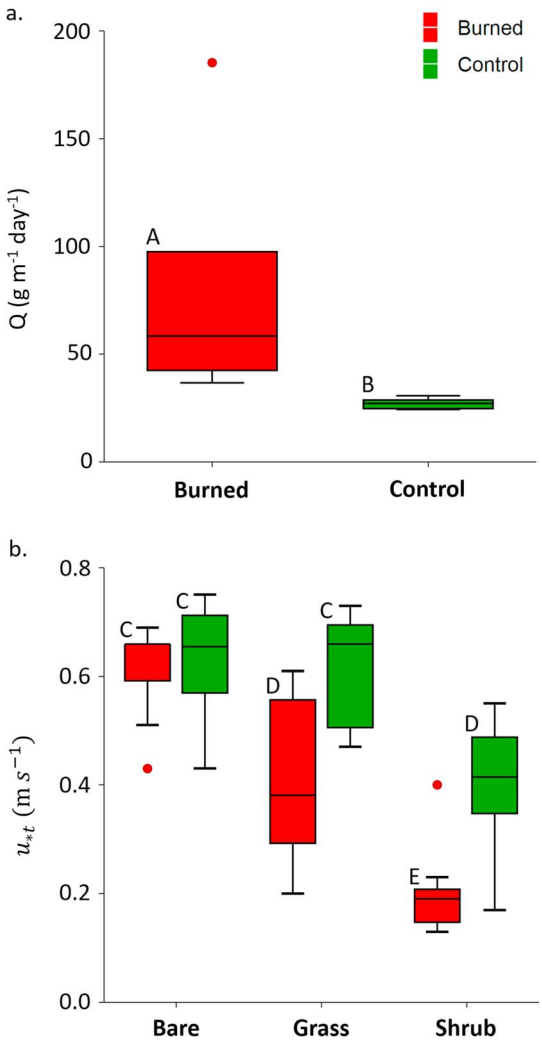

Figure 2. (a) The derived Q from MWAC sediment samplers in the control and burned areas show an average of 27.1 ± 2.4 and 75.3 ± 55.0 g m^{-1} d^{-1}, respectively. The control and burned flux are significantly different as shown by the box plots and the Kruskal-Wallis one-way ANOVA on Ranks statistical test. Significant difference is denoted by the A and B symbols. The red point represents an outlier. (b) The u_{*t} of bare, grass, and shrub sites was derived using measured surface resistances. Grass and shrub u_{*t} decreased significantly following fire and bare sites remained constant as shown by Kruskal-Wallis multiple comparison *Z* value test at a 95% confidence limit. Significant differences are indicated by the differing symbols, C, D, and E. Red points are outliers assuming a normal distribution.

(2 g needed) collected by the control area MWACs, four samples were analyzed, whereas a total of eight samples were analyzed from the burned area MWACs. MWAC samples were taken from collection buckets at the same height and combined to obtain enough mass for the analysis.

REE concentrations were measured using an Inductively Coupled Plasma Optical Emissions Spectrometry (ICP-OES) (Thermo Scientific™ iCAP™ 7000 Series). For this analysis, REEs were leached from the sand, silt, and clay size (< 2 mm) fraction of soil samples using microwave digestion in concentrated HNO_3-HCl (3:1) solution following the US EPA Method 3051A (US EPA, 2007). Soil samples (2.0 g) were placed in microwave digestion tubes followed by 9 mL trace metal grade concentrated HNO_3 and 3 mL concentrated HCl. The samples were allowed to predigest overnight. The microwave digestion process was conducted at 175°C for 30 min then cooled to room temperature. The digested samples were filtered through No. 5 Whatman filter papers and vacuum filtered through 0.45 μm membranes. The filtered samples were diluted to 50 mL for ICP-OES analysis.

To create ternary mixing diagrams, the background REE concentrations were subtracted from the sample REE concentrations and normalized to the average spiked concentration minus the background.

$$N_i = \frac{(C_{Si} - C_{Bi})}{(C_{Ai} - C_{Bi})} \quad (3)$$

$$P_i = \frac{N_i}{\Sigma\left(\frac{C_{Si} - C_{Bi}}{C_{Ai} - C_{Bi}}\right)} \quad (4)$$

where N_i is the is the normalized sample concentration of the *i*th REE tracer, C_{Si} is the concentration of the *i*th tracer in sediment samples, C_{Bi} is the background concentration of the *i*th tracer, and C_{Ai} is the initial spiked concentration of the *i*th tracer applied to the soil surface. Individual normalized sample concentrations were then divided by the sum of all normalized concentrations, yielding the percent of each REE component, P_i.

3. Results

The median total horizontal mass flux (*Q*) for the entire monitoring period (90 days) in the control and burned areas was 27.1 and 58.6 g m^{-1} d^{-1}, respectively (Figure 2a). The mean *Q* was approximately 3 times higher in the burned area than the control, 75.3 ± 55.0 and 27.1 ± 2.4 g m^{-1} d^{-1} respectively. The fitting values of *a*, *b*, and *c* used for equation (1) can be found in Table S1 of the supporting information. Fluxes in the burned area have a much higher variation compared to those of the control area (Figure 2a). Kruskal-Wallis one-way ANOVA on Ranks results indicate that the *Q* was significantly different between the control and burned areas ($p < 0.05$) (Figure 2a).

The u_{*t} estimated from the surface resistance indicate that the microsites differed significantly between the shrub (0.40 ± 0.13 m s^{-1}), grass (0.61 ± 0.11 m s^{-1}), and bare soil (0.63 ± 0.11 m s^{-1}) microsites based on one-way ANOVA ($F = 22.96$, $p < 0.001$) (Figure 2b). The u_{*t} values decreased significantly after the prescribed fire for the shrub (0.20 ± 0.08 m s^{-1}) and grass (0.41 ± 0.14 m s^{-1}) microsites and remained unchanged (0.62 ± 0.08 m s^{-1}) for bare soil based on the Kruskal-Wallis Multiple-Comparison *Z*-Value Test at a 95% confidence limit (Figure 2b).

After the windy season, the proportions of the REEs differed greatly between the sampling zones of control and the burned areas (Figures 3 and 4). Control sampling zones exhibited a mixture of tracers from bare sites

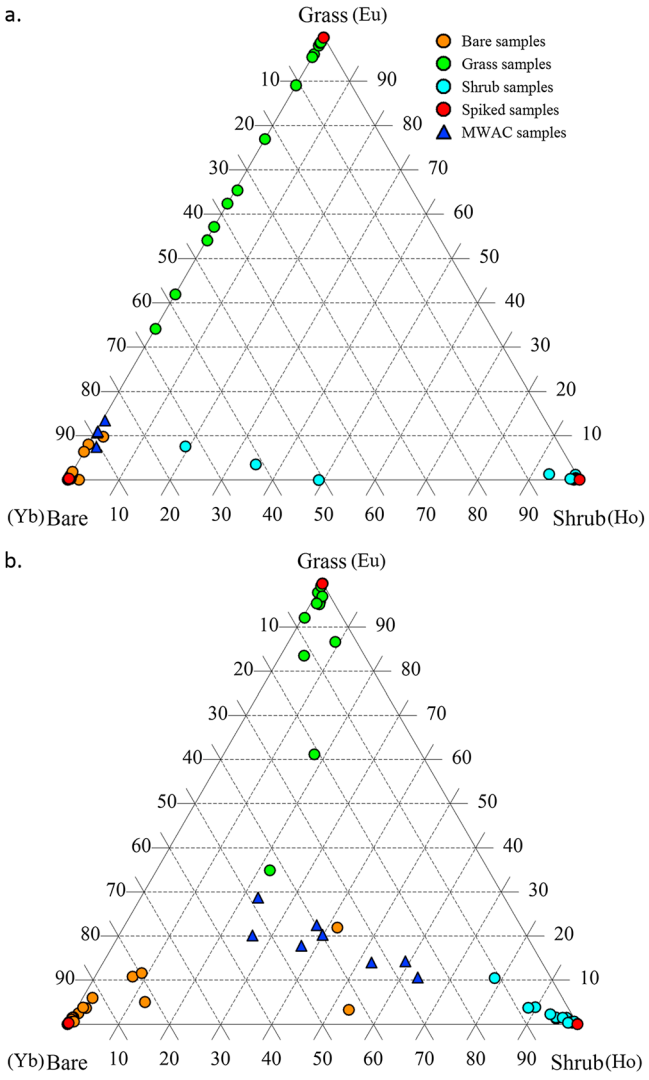

Figure 3. (a) A ternary plot of control area weight percent element composition normalized to the spiked REE concentrations shows mixing between three end members: bare (Yb), grass (Eu), and shrub (Ho). Orange dots display the composition of bare samples after 90 days, green dots are grass samples (90 days), light blue dots are shrub samples (90 days), and the dark blue triangles show the composition of sediment taken from the MWAC samplers. The data points which plot along or near the bare-shrub and bare-grass axes and the dark blue triangles which plot in the bare corner indicate that the main sediment source in the control area is from bare patches, and there is limited sediment mixing between the shrub and grass sites. (b) A ternary plot of the burned area weight percent element composition shows that green and light blue data points plot farther away from the bare-shrub and bare-grass axes, and the dark blue triangles plot predominantly along the bare-shrub axis indicating that the main sediment source is from the bare and shrub patches and that there is mixing between all three microsite types. Red dots at or near the vertices indicate that the initial spiked concentrations of these REE are more than 100 times background values at time zero.

in the vegetated microsites (shrub and grass) (Figure 3a); both grass and shrub microsites were enriched with Yb, the tracer initially applied on the bare interspaces. The sediments from the MWAC samplers in the control replicate plots contained high proportions of the bare microsite tracer and low proportions of vegetative tracer (Yb mean = 88.5 ± 1.7%, Eu mean = 10.7 ± 2.1%, and Ho mean = 0.8 ± 0.6%), compared to those in the burned replicate plots (Yb mean = 39.1 ± 9.3%, Eu mean = 18.5 ± 5.3%, and Ho mean = 42.3 ± 13.8%) (Figures 3a and 3b). In the control sampling zones, there was no significant enrichment of bare sites with tracers initially applied to the vegetated sites (i.e., Ho and Eu) and no exchange of Ho and Eu tracers occurred between the shrub and grass microsites (Table 1 and supporting information Figure S1). The burned sampling zones showed more mixing than the control, with interactions between all three microsite types (Figure 3b). The sediments from the MWAC samplers in the burned replicate plots showed that the Q was predominantly a mixture of shrub-sourced (Ho) and bare-sourced (Yb) sediment, 42.3 ± 13.8% and 39.1 ± 9.3%, respectively. Grass microsites were more enriched with shrub tracer than vice versa (Figure 4).

The bare tracer (Yb) in the bare microsites of the sampling zones showed no significant difference between the spiked (time zero) concentration, the control sampling zone concentration (after 90 days), and the burned sampling zone concentration (after 90 days) at the 95% confidence level (Table 1). However, bare microsites in the burned sampling zone showed a significant increase in the REE tracer concentrations applied under vegetation, Eu and Ho, compared to the background (time zero) concentrations and the control sampling zone concentrations (after 90 days) (Table 1). In the grass microsites a significant increase in Yb tracer, applied to bare interspaces initially, was observed in both the control and burned sampling zones (Table 1). For the grass tracer (Eu), no significant difference was found between the spiked (time zero), control, and burned sampling zones (after 90 days) (Table 1). Finally, for the shrub tracer (Ho), a significant increase was detected in burned sampling zones compared to the control sampling zones and background concentration (Table 1). Shrub microsites followed a similar pattern to the grasses with a significant increase in bare tracer (Yb) concentrations in both the burned and the control sampling zones (Table 1). In addition, a significant increase in grass tracer (Eu) in the shrub sites of the burned sampling zones was observed (Table 1), but no significant difference existed between shrub tracer (Ho) in shrub sites (Table 1). Box plots and statistical analysis ancillary to Table 1 can be found in the supporting information Figure S1.

Meteorological data were gathered for both treatment areas using on-site meteorological towers (Figure 1). Wind direction, speed, precipitation, and soil moisture values can be found in the supporting information (Figures S3–S6).

4. Discussion

Field experiments in a shrub-grass transition zone using aeolian transport monitoring and REE tracers in the Chihuahuan Desert indicate that fires greatly increased the transport and redistribution of sediment by wind. The mean horizontal mass flux of wind-borne sediments was 3 times higher in the burned area compared to the control area. The postfire enhancement of aeolian processes is documented by several other studies and

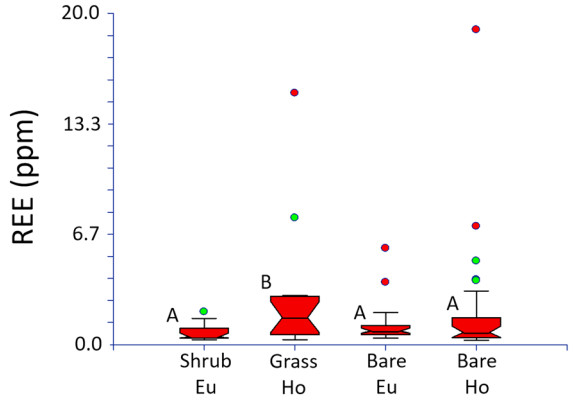

Figure 4. Box plots comparing vegetative tracer (Ho and Eu) concentrations in all three burned zone microsites. Based on the Kruskal-Wallis test, Ho concentrations in the grass site (A) are significantly greater than in the other sites (B). Red points are outliers assuming a normal distribution.

is attributed to the loss of vegetation cover and changes in surface soil properties (e.g., soil water repellency) in the burned area (Miller et al., 2012; Ravi et al., 2012; Sankey et al., 2009; Whicker et al., 2002).

The measured threshold shear velocity u_{*t} for each of the vegetated (shrub and grass) microsites was significantly lower following the fire (both the grass and the shrub microsite u_{*t} decreased by approximately 0.20 m s^{-1}) (Figure 2b). The u_{*t} for the bare microsites did not vary significantly as a function of fire, however, and was greater than the adjacent vegetated microsites. The soil surface of the bare microsites contained more silt and clay and fewer sand particles, more carbonates (inorganic C), and less organic matter (organic *C*) than shrub microsites, and physiochemical (e.g., carbonate-rich) surface crusts could be observed (Figure S2–S7; see also Ravi et al., 2009; Sankey, Ravi, et al., 2012). The shrub and grass microsites also occupy raised microtopographic mound positions, which are erodible roughness elements on the ground surface that are subject to greater erosive force from the wind compared to the relatively flat and smooth bare microsites (Ravi et al., 2009; Sankey, Ravi, et al., 2012). These soil geomorphic differences in the microsite surfaces likely caused the u_{*t} to be higher in the bare, compared to vegetated, microsites. Because the Li et al. (2010) u_{*t} estimation method does not take into account the sheltering effect of the vegetation canopy, the effect of unburned grasses and shrubs on the atmospheric boundary layer—in which vegetation cover acts as a nonerodible roughness element that shelters the soil surface by lowering the surface wind velocity (Ravi et al., 2011; Stockton & Gillette, 1990)—does not contribute to differences in the observed u_{*t} between microsites or between burned and control treatments.

In addition to reducing the protective cover of vegetation, fires can also greatly reduce the threshold shear velocity by decreasing the interparticle bonding forces due to moisture in soils (Li et al., 2007; Ravi et al., 2006). Soil moisture contributes to interparticle cohesive forces either through an adsorption layer or a "liquid bridge" spanning particles (Chepil, 1956; Ravi et al., 2006; Shao, 2008). Fire volatilizes organic compounds in vegetation and surface litter causing, through a strong temperature gradient, the volatilized gasses to be pulled down into the soil column where they condense on the surface of soil particles making them hydrophobic or water repellent (DeBano, 2000). Thus, fires can have a drastic effect on the water content of the soil underneath the differing microsite types, potentially affecting the interparticle moisture bonding forces (adsorption and liquid bridge bonding) which determine u_{*t}. Throughout much of the experiment the burned shrub volumetric water content (VWC) was approximately zero (Figure S6). Experimental studies have shown that water repellent compounds induced by burning vegetation can enhance soil erodibility in dry soils by the effect on soil-water contact angle and on the strength on interparticle wet bonding forces (Ravi et al., 2007). However, fire-induced water repellency in these systems is generally short lived and disappears after the rainy season (Ravi et al., 2009).

The removal of vegetation as a nonerodible roughness element and an associated decrease in VWC following the fire allows for an increase in the surface wind shear as well as a decrease in interparticle cohesive forces which results in greater erosion from shrub and grass sites. Shrub sites also have a lower u_{*t} than that of grass sites. Thus, when vegetation is removed by fire, sediment is more readily entrained and transported from the shrub sites than it is from the grasses. This is supported by the REE concentrations found in the burned area sediment collectors (Figure 3b).

The observed soil resource homogenization resulting from increased sediment transport from previously vegetated, burned microsites have been shown to lead to soil-geomorphic changes in which the spatial patterns of soil properties and microtopography become more evenly distributed (less heterogeneous) across the landscape (Ravi et al., 2009; Sankey et al., 2010; Sankey, Germino, Sankey, & Hoover, 2012; Sankey, Ravi, et al., 2012). The reduction in nonerodible (vegetation) and erodible (microtopography) roughness elements due to burning and postfire erosion alters wind flow and changes geomorphic conditions by more evenly distributing the

Table 1
Mean REE Concentrations Found Within the Differing Microsites Before (spiked) and After the Windy Season in the Control and Burned Treatment Areas

Microsite	Spiked	Control	Burned
Bare Yb (ppm)	248.14	206.13	182.42
Bare Eu (ppm)	0.76	0.99	1.12[a]
Bare Ho (ppm)	0.54	0.92	1.93[a]
Grass Yb (ppm)	1.96[a]	8.50	15.09
Grass Eu (ppm)	95.45	28.49	62.18
Grass Ho (ppm)	0.25	0.211	2.80[a]
Shrub Yb (ppm)	1.24[a]	2.66	5.15
Shrub Eu (ppm)	0.32	0.41	0.75[a]
Shrub Ho (ppm)	164.82	89.22	70.85

[a]A significantly different concentration ($P > 0.05$).

erosive force of wind spatially across the landscape. Such changes in wind flow coupled with postfire changes in the spatial patterns of soil properties mean that the spatially heterogeneous increase in postfire aeolian sediment transport at microsite scales results in the potential loss of microsite and microtopographic variability. This loss of fine-scale landscape heterogeneity renders the soil erodibility and erosivity less spatially variable. The Q is the major flux responsible for local postfire aeolian sediment transport, and typically more than 95% of the flux occurs below the measured 1 m height (Li et al., 2007). As the Q and the amount of saltating particles increases so does the vertical dust flux (F_e) (Gillette et al., 1997; Marticorena & Bergametti, 1995). While F_e was not measured in this experiment, a significant increase in the F_e is generally expected to occur postfire (Van Pelt et al., 2017; Wagenbrenner et al., 2013). A loss of vegetation cover and an increase in aeolian activity do no immediately equate to land degradation; however, if this accelerated sediment transport is sustained by slow vegetation recovery and/or persistent droughts, the landscape may be stripped of nutrients leading to land degradation and an expansion of desert margins (Darkoh, 1998; D'Odorico et al., 2013; Hasselquist et al., 2011; Sankey, Germino, Benner, et al., 2012). Consequences of postfire-accelerated aeolian sediment transport include the following: loss of nutrient-rich fine sediments, damage to postfire vegetation via abrasion (including postfire recovering vegetation and colonizers and/or species planted for restoration), air pollution (tropospheric aerosols), precipitation suppression, and shifts in biogeochemical cycles (Field et al., 2010; Hasselquist et al., 2011; Miller et al., 2012; Ravi et al., 2011; Sankey et al., 2009; Sankey, Germino, Benner, et al., 2012).

The REE tracer analysis of wind-borne sediments showed that Q from the control area was predominantly derived from the bare microsites (88.5 ± 1.7%) (Figure 3). The wind eroded sediments and nutrients are partially redeposited onto vegetated patches by canopy trapping or lost due to long-range transport. This preferential deposition and loss of fine soil and associated nutrients is thought to be a major factor responsible for the formation of shrub islands and deflated bare interspaces leading to land degradation and the expansion of desert margins (D'Odorico et al., 2013; Li et al., 2008; Schlesinger et al., 1990). Thus, the bare soil interspaces in shrub encroached landscapes that are not recently burned act as sediment sources while the vegetated microsites (shrub and grass) act as sinks for the sediments from bare soil sites. Because none of the data points are observed along or near the shrub-grass axis in Figure 3a, the results show limited mixing of sediments between grass and shrub microsites. Furthermore, no significant difference was observed between shrub and grass tracers (Ho and Eu) in bare sites, indicating little or no transport from vegetated microsites under stable (e.g., not recently burned, trampled, or grazed) conditions (Table 1). The burned sampling zones showed greater mixing of sediments occurring between all three microsite types compared to the control sampling zones (Figure 3b). Significant enrichment of each microsite with its two other end members indicates homogenization (i.e., deflation of raised islands of fertility and redistribution onto previously deflated bare interspaces) of sediment following the fire (Table 1). The REE tracer analysis of wind-borne sediments from the burned replicate plots indicates that the Q is primarily composed of particles from the bare and shrub microsites (Figure 3b). These shrub microsites were found to be the most active sediment sources following the fire, which corroborates experiments based on different methods in other burned desert shrublands (Sankey, Germino, & Glenn, 2012). Greater enrichment of shrub tracers in grass microsites than vice versa indicates that the grass microsites became a significant sediment sink following the fire (Figure 4). The grasses are generally fire adapted and typically retain their pedestals with dense fibrous roots which can stabilize the soil particles in grass microsites (Stout, 2012; Van Pelt et al., 2017). Moreover, the postfire recovery of grasses is much faster than shrubs, thereby providing the grasses a competitive advantage in trapping aeolian sediments after fire (Parmenter, 2008; Ravi et al., 2009). This causes sediment from the raised nutrient-rich shrub microsites to be preferentially transported and redistributed to grass and bare microsites, therefore creating a more even, homogenous surface. Resource homogenization is shown to enhance grass regrowth, thus decreasing aeolian transport and associated degradation (Ravi et al., 2009). Thus, the fire-erosion feedbacks can provide a potential negative feedback to shrub encroachment. This study demonstrates that REEs can be used as reliable tracers to identify postfire sinks and sources of sediments and to quantify major components of the Q at the field scale. However, long-term field studies are needed to measure the different resource input and output components to accurately predict postfire sediment redistribution and loss.

Studies in sandy soils have shown that REEs can be preferentially adsorbed to a certain fine fraction of the soil (e.g., Wang et al., 2017; Zhang et al., 2001). Wind preferentially entrains some size fraction of sediment from the soil, which could lead to an overestimation or underestimation of transport (Li et al., 2009). However, in

this study our objective was to compare the relative aeolian sediment transport and spatial redistribution of aeolian sediments in burned and unburned sites. Furthermore, we acknowledge that some disturbances to the surface soil may have inadvertently occurred in both the burned and control plots during the tracer application. Nevertheless, our study represents a useful approach to test the applicability of multiple REE tracers to quantify wind transport and associated soil redistribution at field scale.

Our results support the postfire resource redistribution and landscape homogenization hypothesized and tested by several studies (Ravi et al., 2009; Sankey et al., 2010; Sankey, Germino, Sankey, & Hoover, 2012; White et al., 2006). In particular, our study clearly demonstrated postfire homogenization and more importantly identified sediment sources and sinks. Thus, fires in the early stages of the shrub-grass transition can provide an important feedback mechanism to combat this process. However, as observed in our study, fires can greatly accelerate the sediment transport by wind and possibly subsequent dust emissions (Figure 2). Hence, the timing of fire and postfire climatic conditions are important factors controlling the balance between sediment loss and redistribution. For example, if fires are followed by persistent droughts or extreme winds, the ecosystem might experience a net loss of resources rather than redistribution, resulting in a completely deflated surface devoid of vegetation (Sankey, Germino, Sankey, & Hoover, 2012). Such changes can fundamentally alter the geomorphology by making soil erodibility and erosivity less spatially variable and making more of the total landscape area both a potential source and sink for sediment transport. Moreover, in some systems, the homogenization can have undesirable environmental consequences. For instance, in the cold desert sagebrush steppe of the Great Basin, USA, desirable shrubs may not recover postfire due to the positive feedbacks between fire, erosion, invasive annual grasses, and landscape homogenization (Sankey, Germino, Sankey, & Hoover, 2012).

5. Conclusion

Using a unique multiple tracer-based approach, our findings directly address key questions regarding how interactions among fire, wind, vegetation, and soil processes in a shrub-grass transition ecosystem affect aeolian transport. We tested the field applicability of a potentially valuable tracer technique, REE tracers for aeolian transport studies, which could be used to monitor landscape responses to disturbances, components of aeolian fluxes, as well as sediment sources and sinks. In our study, while fires are seen to dramatically increase sediment transport and nutrient loss, they can also, through a shift in u_{*t} under varying microsite types, induce micotopographic changes associated with differing vegetation types. Aeolian sediment sources and sinks are altered following fires, allowing for homogenization of surface sediment which may be trapped by the vegetation. These processes are thought to enhance grass regrowth by providing a negative feedback mechanism to woody plant encroachment and reversing associated heterogeneous surface. As climate change progresses, a potential increase in aridity in drylands may increase the frequency and intensity of fires, along with acceleration of soil erosion processes and a prolonged postfire window of soil erosion disturbances. Considering the extent of degrading dryland ecosystems currently experiencing both hydrologic- and aeolian-accelerated sediment transport (87% of the world's degrading drylands) understanding the interactions among vegetation dynamics, disturbance and soil erosion are critical. Our study presents a first step toward developing a valuable tool to monitor the ecogeomorphic response of these landscapes to changing climate, disturbance, and management scenarios.

Acknowledgments
This research was funded by the U.S. National Science Foundation (NSF) Award EAR-1451518 for S. Ravi, Award EAR 1451489 for J. Li, and the Sevilleta LTER Graduate Student Summer Fellowship for D. Dukes. The authors gratefully acknowledge the contributions of Jon Erz, Eric Krueger and Andy Lopez (FWS, SNWR) and Scott Collins, Renée Brown and Amaris Swan (Sevilleta LTER, New Mexico, USA) for providing access to field and laboratory facilities and technical guidance. Both the data from the experiments and input files necessary to reproduce the figures are included as a supporting information to the manuscript. Any use of trade, product, or firm names is for descriptive purposes only and does not imply endorsement by the U.S. government. USDA is an equal opportunity provider and employer.

References

Archer, S., Schimel, D. S., & Holland, E. A. (1995). Mechanisms of shrubland expansion: Land use, climate or CO_2? *Climatic Change*, *29*(1), 91–99. https://doi.org/10.1007/BF01091640

Báez, S., & Collins, S. L. (2008). Shrub invasion decreases diversity and alters community stability in northern Chihuahuan desert plant communities. *PLoS One*, *3*(6). https://doi.org/10.1371/journal.pone.0002332

Bhattachan, A., D'Odorico, P., Okin, G. S., & Dintwe, K. (2013). Potential dust emissions from the southern Kalahari's dunelands. *Journal of Geophysical Research: Earth Surface*, *118*, 307–314. https://doi.org/10.1002/jgrf.20043

Bowman, M., Balch, J. K., Artaxo, P., Bond, W. J., Carlson, J. M., Cochrane, M. A., … Pyne, S. J. (2009). Fire in the Earth system. *Science*, *324*(5926), 481–484. https://doi.org/10.1126/science.1163886

Chepil, W. S. (1956). Influence of moisture on erodibility by wind. *Soil Science Society of America Journal*, *20*(2), 288–292. https://doi.org/10.2136/sssaj1956.03615995002000020033x

Darkoh, M. B. K. (1998). The nature, causes and consequences of desertification in the drylands of Africa. *Land Degradation & Development*, *9*(1), 1–20. https://doi.org/10.1002/(SICI)1099-145X(199801/02)9:1<1::AID-LDR263>3.0.CO;2-8

Deasy, C., & Quinton, J. N. (2010). Use of rare earth oxides as tracers to identify sediment source areas for agricultural hillslopes. *Solid Earth*, *1*(1), 111–118. https://doi.org/10.5194/se-1-111-2010

DeBano, L. F. (1966). Formation of non-wettable soils: Involves heat transfer mechanism. In *Pacific Southwest Forest and Range Experiment Station* (Vol. 132). Pacific Southwest Forest & Range Experiment Station.

Debano, L. F. (2000). The role of fire and soil heating on water repellency in wildland environments: A review. *Journal of Hydrology*, *231*(2000), 195–206.

D'Odorico, P., Bhattachan, A., Davis, K. F., Ravi, S., & Runyan, C. W. (2013). Global desertification: Drivers and feedbacks. *Advances in Water Resources*, *51*, 326–344. https://doi.org/10.1016/j.advwatres.2012.01.013

Field, J. P., Belnap, J., Breshears, D. D., Neff, J. C., Okin, G. S., Whicker, J. J., … Reynolds, R. L. (2010). The ecology of dust. *Frontiers in Ecology and the Environment*, *8*(8), 423–430. https://doi.org/10.1890/090050

Gillette, D. A., Fryrear, D. W., Gill, T. E., Ley, T., Cahill, T. A., & Gearhart, E. A. (1997). Relation of vertical flux of particles smaller than 10 μm to total aeolian horizontal mass flux at Owens Lake. *Journal of Geophysical Research*, *102*, 26,009–26,015. https://doi.org/10.1029/97JD02252

Gillette, D. A., & Pitchford, A. M. (2004). Sand flux in the northern Chihuahuan desert, New Mexico, USA, and the influence of mesquite-dominated landscapes. *Journal of Geophysical Research*, *109*, F04003. https://doi.org/10.1029/2003JF000031

Guzmán, G., Quinton, J. N., Nearing, M. A., Mabit, L., & Gómez, J. A. (2013). Sediment tracers in water erosion studies: Current approaches and challenges, *J. Soils Sediments*, *13*(4), 816–833. https://doi.org/10.1007/s11368-013-0659-5

Hasselquist, N. J., Germino, M. J., Sankey, J. B., Ingram, L. J., & Glenn, N. F. (2011). Aeolian nutrient fluxes following wildfire in sagebrush steppe: Implications for soil carbon storage. *Biogeosciences*, *8*, 3649–3659. https://doi.org/10.5194/bg-8-3649-2011

Haxel, G. B., Hedrick, J. B., Orris, G. J., Stauffer, P. H., & Hendley, J. W. II (2002). Rare earth elements: Critical resources for high technology. *United States Geological Survey's Fact Sheet*, *87–2*, 4.

Higgins, R. W., Yao, Y., & Wang, X. L. (1997). Influence of the North American monsoon system on the US summer precipitation regime. *Journal of Climate*, *10*(10), 2600–2622. https://doi.org/10.1175/1520-0442(1997)010<2600:IOTNAM>2.0.CO;2

Huxman, T. E., Wilcox, B. P., Breshears, D. D., Scott, R. L., Snyder, K. A., Small, E. E., … Jackson, R. B. (2005). Ecohydrological implications of woody plant encroachment. *Ecology*, *86*(2), 308–319. https://doi.org/10.1890/03-0583

Johnson, W. R. (1988). Soil survey of Socorro county area, New Mexico. USDA soil conservation service, in cooperation with USDI BLM and BIA, and NM agricultural experiment station. Retrieved from https://www.nrcs.usda.gov/Internet/FSE_MANUSCRIPTS/new_mexico/NM664/0/Socorro.pdf. 13 January, 2017. https://doi.org/10.1207/s15326888chc1702_7

Kimoto, A., Nearing, M. A., Zhang, X. C., & Powell, D. M. (2006). Applicability of rare earth element oxides as a sediment tracer for coarse-textured soils. *Catena*, *65*(3), 214–221. https://doi.org/10.1016/j.catena.2005.10.002

Lal, R. (2001). Soil degradation by water erosion. *Land Degradation & Development*, *12*(6), 519–539. https://doi.org/10.1002/ldr.472

Li, J., Okin, G. S., Alvarez, L., & Epstein, H. (2007). Quantitative effects of vegetation cover on wind erosion and soil nutrient loss in a desert grassland of southern New Mexico, USA. *Biogeochemistry*, *85*, 317–332. https://doi.org/10.1007/s10533-007-9142-y

Li, J., Okin, G. S., Alvarez, L., & Epstein, H. (2008). Effects of wind erosion on the spatial heterogeneity of soil nutrients in two desert grassland communities. *Biogeochemistry*, *88*(1), 73–88. https://doi.org/10.1007/s10533-008-9195-6

Li, J., Okin, G. S., & Epstein, H. E. (2009). Effects of enhanced wind erosion on surface soil texture and characteristics of windblown sediments. *Journal of Geophysical Research*, *114*, G02003. https://doi.org/10.1029/2008JG000903

Li, J., Okin, G. S., Herrick, J. E., Belnap, J., Miller, M. E., Vest, K., & Draut, A. E. (2013). Evaluation of a new model of aeolian transport in the presence of vegetation. *Journal of Geophysical Research: Earth Surface*, *118*, 288–306. https://doi.org/10.1002/jgrf.20040

Li, J., Okin, G. S., Herrick, J. E., Belnap, J., Munson, S. M., & Miller, M. E. (2010). A simple method to estimate threshold friction velocity of wind erosion in the field. *Geophysical Research Letters*, *37*, L10402. https://doi.org/10.1029/2010GL043245

Marticorena, B., & Bergametti, G. (1995). Modeling the atmospheric dust cycle: 1. Design of a soil-derived dust emission scheme. *Journal of Geophysical Research*, *100*(D8), 16,415–16,430. https://doi.org/10.1029/95JD00690

Mayaud, J. R., Bailey, R. M., & Wiggs, G. F. (2017). A coupled vegetation/sediment transport model for dryland environments. *Journal of Geophysical Research: Earth Surface*, *122*, 875–900. https://doi.org/10.1002/2016JF004096

McPherson, G. R. (1995). The role of fire in the desert grasslands. In M. P. McClaran & T. T. Van Devender (Eds.), *The desert grassland* (pp. 130–151). Tucson: University of Arizona Press.

Middleton, N., & Thomas, D. (1997). World atlas of desertification., Arnold, Hodder Headline, PLC, No. Ed. 2.

Millennium Ecosystem Assessment (2005). *Ecosystems and human well-being: Desertification synthesis*. Washington, DC: World Resources Institute: Island Press.

Miller, M. E., Bowker, M. A., Reynolds, R. L., & Goldstein, H. L. (2012). Postfire land treatments and wind erosion—Lessons from the Milford Flat fire, UT, USA. *Aeolian Research*, *7*, 29–44. https://doi.org/10.1016/j.aeolia.2012.04.001

Munson, S. M., Belnap, J., & Okin, G. S. (2011). Responses of wind erosion to climate induced vegetation changes on the Colorado Plateau. *Proceedings of the National Academy of Sciences of the United States of America*, *108*, 3854–3859. https://doi.org/10.1073/pnas.1014947108

NCSS (2016). Statistical Software [Computer software]. Retrieved from https://www.ncss.com/download/ncss/updates/ncss-11/

Okin, G. S., & Gillette, D. A. (2001). Distribution of vegetation in wind-dominated landscapes: Implications for wind erosion modeling and landscape processes. *Journal of Geophysical Research*, *106*(D9), 9673–9683. https://doi.org/10.1029/2001JD900052

Parmenter, R. R. (2008). Long-term effects of a summer fire on desert grassland plant demographics in New Mexico. *Rangeland Ecology & Management*, *61*(2), 156–168. https://doi.org/10.2111/07-010.1

Paysen, T. E., Ansley, R. J., Brown, J. K., Gottfried, G. J., Haase, S. M., Harrington, M. G., … Wilson, R. C. (2000). Fire in western shrubland, woodland, and grassland ecosystems. *USDA Forest Service General Technical Report*, *2*, 121–159.

Polyakov, V. O., & Nearing, M. A. (2004). Rare earth element oxides for tracing sediment movement. *Catena*, *55*, 255–276. https://doi.org/10.1016/S0341-8162(03)00159-0

Ravi, S., Baddock, M. C., Zobeck, T. M., & Hartman, J. (2012). Field evidence for differences in post-fire aeolian transport related to vegetation type in semi-arid grasslands. *Aeolian Research*, *7*, 3–10. https://doi.org/10.1016/j.aeolia.2011.12.002

Ravi, S., & D'Odorico, P. (2009). Post-fire resource redistribution and fertility island dynamics in shrub encroached desert grasslands: A modeling approach. *Landscape Ecology*, *24*(3), 325–335. https://doi.org/10.1007/s10980-008-9307-7

Ravi, S., D'Odorico, P., Breshears, D. D., Field, J. P., Goudie, A. S., Huxman, T. E., … Zobeck, T. M. (2011). Aeolian processes and the biosphere. *Reviews of Geophysics*, *49*, RG3001. https://doi.org/10.1029/2010RG000328

Ravi, S., D'Odorico, P., Wang, L., White, C. S., Okin, G. S., Macko, S. A., & Collins, S. L. (2009). Post-fire resource redistribution in desert grasslands: A possible negative feedback on land degradation. *Ecosystems*, *12*(3), 434–444. https://doi.org/10.1007/s10021-009-9233-9

Ravi, S., D'Odorico, P., Zobeck, T. M., Over, T. M., & Collins, S. L. (2007). Feedbacks between fires and wind erosion in heterogeneous arid lands. *Journal of Geophysical Research*, *112*, G04007. https://doi.org/10.1029/2007JG000474

Ravi, S., Zobeck, T. M., Over, T. M., Okin, G. S., & D'Odorico, P. (2006). On the effect of moisture bonding forces in air-dry soils on threshold friction velocity of wind erosion. *Sedimentology*, *53*(3), 597–609. https://doi.org/10.1111/j.1365-3091.2006.00775.x

Retta, A., Armbrust, D. V., Hagen, L. J., & Skidmore, E. L. (2000). Leaf and stem area relationships to masses and their height distributions in native grasses. *Agronomy Journal*, *92*(2), 225–230. https://doi.org/10.2134/agronj2000.922225x

Sankey, J. B., Germino, M. J., Benner, S. G., Glenn, N. F., & Hoover, A. N. (2012). Transport of biologically important nutrients by wind in an eroding cold desert. *Aeolian Research*, *7*, 17–27. https://doi.org/10.1016/j.aeolia.2012.01.003

Sankey, J. B., Germino, M. J., & Glenn, N. F. (2009). Eolian sediment transport following wildfire in sagebrush steppe. *Journal of Arid Environments*, *73*(10), 912–919. https://doi.org/10.1016/j.jaridenv.2009.03.016

Sankey, J. B., Germino, M. J., & Glenn, N. F. (2012). Dust supply varies with sagebrush microsites and time since burning in experimental erosion events. *Journal of Geophysical Research*, *117*, G01013. https://doi.org/10.1029/2011JG001724

Sankey, J. B., Germino, M. J., Sankey, T. T., & Hoover, A. (2012). Fire effects on the spatial patterning of soil properties in sagebrush steppe, USA: Meta-analysis. *International Journal of Wildland Fire*, *21*(5), 545–556. https://doi.org/10.1071/WF11092

Sankey, J. B., Glenn, N. F., Germino, M. J., Gironella, A. I. N., & Thackray, G. D. (2010). Relationships of aeolian erosion and deposition with LiDAR-derived landscape surface roughness following wildfire. *Geomorphology*, *119*, 135–145. https://doi.org/10.1016/j.geomorph.2010.03.013

Sankey, J. B., Law, D., Breshears, D. D., Munson, S. M., & Webb, R. H. (2013). Employing LiDAR to detail vegetation canopy architecture for prediction of aeolian transport. *Geophysical Research Letters*, *40*, 1724–1728. https://doi.org/10.1002/grl.50356

Sankey, J. B., Ravi, S., Wallace, C. S. A., Webb, R. H., & Huxman, T. E. (2012). Quantifying soil surface change in degraded drylands: Shrub encroachment and effects of fire and vegetation removal in a desert grassland. *Journal of Geophysical Research*, *117*, G02025. https://doi.org/10.1029/2012JG002002

Schlesinger, W. H., Reynolds, J. F., Cunningham, G. L., Huenneke, L. F., Jarrell, W. M., Virginia, R. A., & Whitford, W. G. (1990). Biological feedbacks in global desertification. *Science*, *247*, 1043–1048. https://doi.org/10.1126/science.247.4946.1043

Shao, Y. (2008). *Physics and modeling of wind erosion* (Vol. 37). Heidelberg: Springer Science and Business Media.

Shao, Y., & Raupach, M. R. (1992). The overshoot and equilibration of saltation. *Journal of Geophysical Research*, *97*(D18), 20,559–20,564. https://doi.org/10.1029/92JD02011

Shao, Y., Raupach, M. R., & Findlater, P. A. (1993). Effect of saltation bombardment on the entrainment of dust by wind. *Journal of Geophysical Research*, *98*(D7), 12,719–12,726. https://doi.org/10.1029/93JD00396

Stockton, P. H., & Gillette, D. A. (1990). Field measurment of the shelting effect of vegetation on erodable land surfaces. *Land Degradation & Development*, *2*(2), 77–85. https://doi.org/10.1002/ldr.3400020202

Stout, J. E. (2012). A field study of wind erosion following a grass fire on the Llano Estacado of North America. *Journal of Arid Environments*, *82*, 165–174. https://doi.org/10.1016/j.jaridenv.2012.02.001

Turnbull, L., Wilcox, B. P., Belnap, J., Ravi, S., D'Odorico, P., Childers, D., … Caylor, K. K. (2012). Understanding the role of ecohydrological feedbacks in ecosystem state change in drylands. *Ecohydrology*, *5*(2), 174–183. https://doi.org/10.1002/eco.265

United Nations Convention to Combat Desertification (1994). United Nations Convention to Combat Desertification in Countries Experiencing Serious Drought And/or Desertification, Particularly in Africa. A/ AC.241/27, (September), 1–58. Retrieved from http://www.unccd.int/convention/menu.php. 15 January, 2017.

US EPA (United States Environmental Protection Agency) (2007). SW-846 test method 3051A. Revision 1. Microwave assisted acid digestion of sediments, sludges, soils, and oils. Washington, DC: United States Environmental Protection Agency. https://www.epa.gov/hw-sw846/sw-846-test-method-3051a-microwave-assisted-acid-digestion-sediments-sludges-soils-and-oils, accessed 15 January, 2017.

Van Auken, O. W. (2000). Shrub invasions of North American semiarid grasslands. *Annual Review of Ecology and Systematics*, *31*(1), 197–215. https://doi.org/10.1146/annurev.ecolsys.31.1.197

Van Pelt, R. S., Baddock, M. C., Barnes, M. C. W., Strack, J. E., & Zobeck, T. M. (2012). Use of rare earth elements in investigations of aeolian processes. *Eos, Transactions American Geophysical Union*, *1*(03), Fall Meet. Suppl. Abstract A42E-03. https://doi.org/10.1186/1546-0096-10-27

Van Pelt, R. S., Baddock, M. C., Zobeck, T. M., D'Odorico, P., Ravi, S., & Bhattachan, A. (2017). Total vertical sediment flux and PM10 emissions from disturbed Chihuahuan Desert surfaces. *Geoderma*, *293*, 19–25. https://doi.org/10.1016/j.geoderma.2017.01.031

Van Pelt, R. S., & Zobeck, T. M. (2007). Chemical constituents of fugitive dust. *Environmental Monitoring and Assessment*, *130*(1–3), 3–16.

Van Pelt, R. S., Barnes, M. C. W., Baddock, M. C., D'Odorico, P., Li, J., Okin, G. S., & Zobeck, T. M. (2014). *Using rare earth element tracers to investigate aeolian processes*. Paper presented at 8th International Confrence of Aeolian Research, Proc. Eighth Int. Conf. Aeolian Res., Lanzhou, China.

Wagenbrenner, N. S., Germino, M. J., Lamb, B. K., Robichaud, P. R., & Foltz, R. B. (2013). Wind erosion from a sagebrush steppe burned by wildfire: Measurments of PM_{10} and total horizontal sediment flux. *Aeolian Research*, *10*, 25–36. https://doi.org/10.1016/j.aeolia.2012.10.003

Wang, G., Li, J., Ravi, S., Van Pelt, R. S., Costa, P. J., & Dukes, D. (2017). Tracer techniques in aeolian reseach: Approaches, applications, and challenges. *Earth-Science Reviews*, *170*, 1–16. https://doi.org/10.1016/J.EARSCIREV.2017.05.001

Whicker, J. J., Breshears, D. D., Wasiolek, P. T., Kirchner, T. B., Tavani, R. A., Schoep, D. A., & Rodgers, J. C. (2002). Temporal and spatial variation of episodic wind erosion in unburned and burned semiarid shrubland. *Journal of Environmental Quality*, *31*(2), 599. https://doi.org/10.2134/jeq2002.0599

White, C. S., Pendleton, R. L., & Pendleton, B. K. (2006). Response of two semiarid grasslands to a second fire application. *Rangeland Ecology & Management*, *59*(1), 98–106. https://doi.org/10.2111/04-153R2.1

White, J. D., & Swint, P. (2014). Fire effects in the northern Chihuahuan Desert derived from Landsat-5 Thematic Mapper spectral indices. *8*(1), 83,667. https://doi.org/10.1117/1.JRS.8.083667

Zhang, X. C., Friedrich, J. M., Nearing, M. A., & Norton, L. D. (2001). Potential use of rare earth oxides as tracers for soil erosion and aggregation studies. *Soil Science Society of America Journal*, *65*, 1508. https://doi.org/10.2136/sssaj2001.6551508x

Zhu, M., Tan, S., Dang, H., & Zhang, Q. (2011). Rare earth elements tracing the soil erosion processes on slope surface under natural rainfall. *Journal of Environmental Radioactivity*, *102*(12), 1078–1084. https://doi.org/10.1016/j.jenvrad.2011.07.007